REPORT DOCUMENTATION PAGE

Form Approved
OMB No. 0704-0188

1. REPORT DATE *(DD-MM-YYYY)*	**2. REPORT TYPE**	**3. DATES COVERED** *(From - To)*
March 2012	Technical Paper	March 2012-July 2012

4. TITLE AND SUBTITLE
Modeling of Neutral Entrainment in an FRC Thruster

5a. CONTRACT NUMBER
In-House

5b. GRANT NUMBER

5c. PROGRAM ELEMENT NUMBER

6. AUTHOR(S)

J. Brackbill, N. Gimelshein, S. Gimelshein, J.-L. Cambier, A. Ketsdever

5d. PROJECT NUMBER

5e. TASK NUMBER

5f. WORK UNIT NUMBER
23041057

7. PERFORMING ORGANIZATION NAME(S) AND ADDRESS(ES)

Air Force Research Laboratory (AFMC)
AFRL/RQRS
1 Ara Drive.
Edwards AFB CA 93524-7013

8. PERFORMING ORGANIZATION REPORT NO.

9. SPONSORING / MONITORING AGENCY NAME(S) AND ADDRESS(ES)
Air Force Research Laboratory (AFMC)
AFRL/RQR
5 Pollux Drive
Edwards AFB CA 93524-7048

10. SPONSOR/MONITOR'S ACRONYM(S)

11. SPONSOR/MONITOR'S REPORT NUMBER(S)
AFRL-RZ-ED-TP-2012-205

12. DISTRIBUTION / AVAILABILITY STATEMENT
Distribution A: Approved for Public Release; Distribution Unlimited. PA#12467

13. SUPPLEMENTARY NOTES
Conference paper for the 28th International Symposium on Rarefied Gas Dynamics, Zaragoza, Spain, 9-13 July 2012.

14. ABSTRACT
Neutral entrainment in a field reversed configuration thruster is modeled numerically with an implicit PIC code extended to include thermal and chemical interactions between plasma and neutral particles. The contribution of charge exchange and electron impact ionization reactions is analyzed, and the sensitivity of the entrainment efficiency to the plasmoid translation velocity and neutral density is evaluated.

15. SUBJECT TERMS

16. SECURITY CLASSIFICATION OF:			**17. LIMITATION OF ABSTRACT**	**18. NUMBER OF PAGES**	**19a. NAME OF RESPONSIBLE PERSON**
					Jean-Luc Cambier
a. REPORT	**b. ABSTRACT**	**c. THIS PAGE**			**19b. TELEPHONE NO** *(include area code)*
Unclassified	**Unclassified**	**Unclassified**	SAR	10	661-275-5649

Standard Form 298 (Rev. 8-98)
Prescribed by ANSI Std. 239.18

Modeling of Neutral Entrainment in an FRC Thruster

Jeremiah Brackbill*, Natalia Gimelshein*, Sergey Gimelshein*, Jean-Luc Cambier† and Andrew Ketsdever†

*ERC, Inc., Edwards AFB, CA 9352
†Propulsion Directorate, Edwards AFB, CA 93524

Abstract. Neutral entrainment in a field reversed configuration thruster is modeled numerically with an implicit PIC code extended to include thermal and chemical interactions between plasma and neutral particles. The contribution of charge exchange and electron impact ionization reactions is analyzed, and the sensitivity of the entrainment efficiency to the plasmoid translation velocity and neutral density is evaluated.

Keywords: field reversed configuration propulsion, neutral entrainment
PACS: 52.75.Di, 52.55.Lf, 52.65.Rr

INTRODUCTION

High-power electric propulsion is an enabling technology for future space missions, but one that also presents a number of technical challenges. First, it is critically important to operate a thruster at very high efficiency, otherwise the system limitations due to heat rejection become insurmountable. Second, high power can be efficiently delivered into a plasma by raising its temperature (provided radiative losses are not excessive), i.e. its specific energy; consequently, the specific impulse can take large values, even in the excess of 10,000 sec. The optimal conditions from the standpoint of low radiation loss, acceptable ionization cost, and confinement requirements, are usually achieved for low-Z plasma at high (50-100 eV) temperature and in strong magnetic fields. These conditions are typically obtained in Field Reversed Configuration (FRC) plasma (see, for example, Ref. [1]). The FRC is a self-organized magnetized plasma structure in the shape of a highly compact toroid. The magnetic field is mostly in the poloidal direction [2], generated by internal (toroidal) currents.

In contrast to some other high I_{sp} plasma propulsion concepts [3], the FRC is completely magnetically insulated from the external field: the plasma is not tied to an external field line, and the FRC can readily detach from the confining external field. It can also be translated and accelerated by applying a gradient of magnetic pressure using pulsed external coils. The FRC can therefore be efficiently accelerated to provide thrust, operates at a temperature that is optimal for ionization and is well confined. The basic concept of operations has been demonstrated by Kirtley et al. [4], and more recent research has led to further optimization of the formation process [5], while methods for increased efficiency through energy recovery in the electrical circuits are currently being developed. One of the latest design iterations [6] provides plasma velocities in the 10-40 km/sec range, a desirable regime for many propulsion applications. However, many aspects of the flow development and device operation, such as power and mass utilization efficiencies, still remain to be determined more precisely.

One of the key features of a versatile FRC thruster is its ability to increase thrust level and operational efficiency through the process of entrainment of neutral (and possibly ambient) gas by a translating FRC plasmoid. The main idea of such an entrainment is the interaction of fast ions with slow neutrals, subsequent charge exchange reactions, and the creation of slow ions and fast neutrals. Fast neutrals will then exit the thruster and produce thrust, while slow ions may again be accelerated. The repetition of this process will allow drastic reduction of energy loss on ionization, while gaining thrust through multiple collisions of accelerated ions with slow neutrals. A significant problem that may reduce the usefullness of the neutral entrainment is the electron impact ionization reactions. These reactions may not just reduce the benefits of entrainment, but potentially degrade thruster efficiency and diminish the usefulness of the neutral entrainment.

In this work, the relative importance of the electron impact ionization and charge exchange reactions is analyzed numerically. First, the balance between ionization and charge exchange reaction rates is examined for various gases and temperatures. Then, a study of heat bath relaxation is performed and the impact of Coulomb collisions is clarified. Finally, a Celeste3D particle-in-cell computational tool [7], extended to include the interactions between the charged

and neutral particles and neutral particle transport, as well as Coulomb interactions between charged particles, is used in simulations of an FRC plasmoid and neutral gas interaction.

ELECTRON IMPACT IONIZATION AND CHARGE EXCHANGE RATES

Prior to modeling the reaction processes in plasma due to the presence of neutral atoms, let us examine the reaction rates of these processes for different gases in the range of temperatures typical for an FRC thruster [8]. Consider first the reaction processes in light gas, helium. The reaction rates as function of temperature are shown in Fig. 1 (left). Note that in addition to the electron impact ionization (denoted EII in the figure) and single charge exchange (SCX) reactions, the total recombination reaction rate is shown. Mechanisms for recombination include the radiative recombination in three-body collisions ($A^+ + e + e \rightarrow A + e$) and the radiative photorecombination ($A^+ + e \rightarrow A + h\nu$). For the recombination reactions, an ion and electron number density of 10^{18} m^{-3} is assumed, similar to that observed in experiments of Ref. [4].

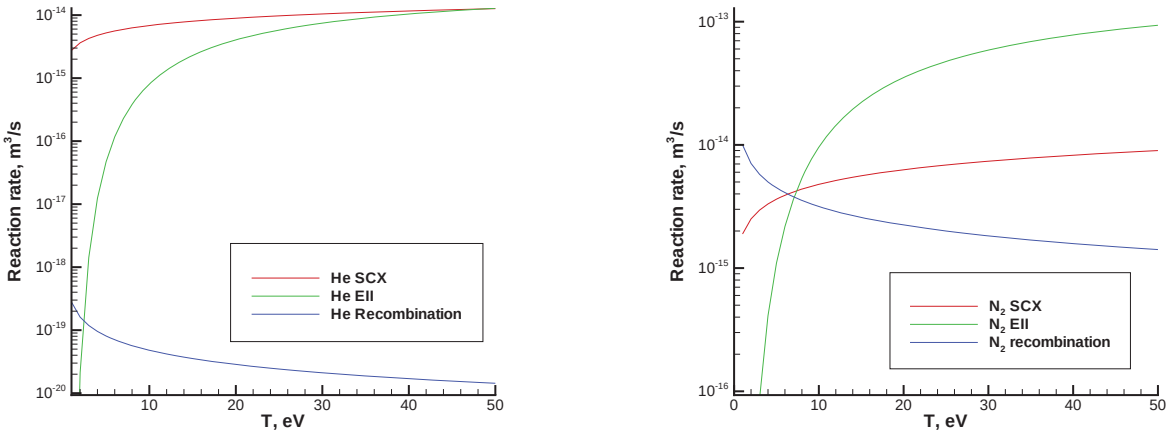

FIGURE 1. Different reaction rates in helium (left) and molecular nitrogen (right).

The electron impact ionization rates k_{eii} presented in this work are obtained by the integration of the translational energy-dependent cross sections σ_{eii} tabulated in SIGLO database [9] as

$$k_{eii} = \int g\sigma_{eii}(g)\, f_e(g)\mathrm{d}g, \tag{1}$$

where g is the relative collision velocity and f_e is the Maxwellian distribution function. For the charge exchange reactions, an expression from [10] is used for the reaction cross section, written in CGS units as

$$\sigma_{scx} = \begin{cases} 0.5\pi a_0^2 \frac{Ry}{E_i} \log^2\left(100\sqrt{\frac{E_i}{\varepsilon}\frac{\mu}{m_e}}\right) & \varepsilon \geq \varepsilon^* \\ \pi\sqrt{\alpha e^2/2\varepsilon} & \varepsilon < \varepsilon^* \end{cases} \tag{2}$$

integrated to obtain the reaction rate similar to Eq. 1. Here,

$$\varepsilon^* = \frac{2\alpha e^2}{a_0^4}\frac{E_i^2}{Ry^2}\left(\log\left(100\sqrt{\frac{E_i}{\varepsilon^*}\frac{\mu}{m_e}}\right)\right)^{-4} \tag{3}$$

is a transcendental equation for ε^*, a_0 is the Bohr radius, E_i is the ionization energy, m and μ are particle mass and reduced mass, respectively, and α is the polarizability. For the recombination reaction rates, the expressions from [11] are used, which are, for the photorecombination, $k_{r1} = 2.7\times10^{-19}T_e^{-0.75}$ (m^3/s), and for the three-body recombination $k_{r2} = 8.75\times10^{-39}T_e^{-4.5}n_e$ (m^3/s)

According to [4, 8], the plasmoid temperature is expected to be less than 50 eV, and in some cases may cool to as low as 5 eV. It is clear from Fig. 1 (left) that at those temperatures and a number density on the order of 10^{18} m-3,

the recombination is not important. The ionization reaction rate is lower than the charge exchange rate, which may be an indication that the entrainment process in a helium-based FRC thruster may be expected to be fairly efficient, especially for lower plasma temperatures. Note however that for temperatures below 10 eV and a typical plasmoid-neutral interaction time of 50 μs, the fraction of ions that participate in a charge exchange reactions may be as low as 10% when the neutral density does not exceed 10^{18} m$-$3. A higher neutral density will therefore be required to increase the number of charge exchange reactions and thus the efficiency of the entrainment process.

Even though the relationship between the ionization and charge exchange reactions is favorable for helium, the thrust level of a helium-based thruster is relatively low, and using a heavier species may therefore be attractive. One of potential candidates could be nitrogen, especially keeping in mind its airbreathing potential. The charge exhange, ionization, and recombination rates for nitrogen are shown in Fig. 1 (right). Note that for recombination rate, the dissociative recombination process ($A_2^- + e \rightarrow A + A^*$) is also included, that is the fastest mechanism of bulk recombination for molecules, with a rate of $k_{r3} = 1.0 \times 10^{-13} T_e^{-0.5} m^3/s$. It can be seen that the plasmoid translation and entrainment is expected to be dominated by recombination at temperatures below $\sim$5 eV and by the electron impact ionization at higher temperatures. The latter one is related to a relatively low iniozation threshold of 15.6 eV as compared to the average energy in translational and internal modes of molecular nitrogen, The charge exchange reactions are expected to be significantly less frequent than the other two processes at all temperatures, and thus it may be diffucult to achieve high efficiency in a nitrogen-based FRC thruster.

An atomic species with a fairly high ionization energy of 21.6 eV is neon. The charge exchange and ionization rates for neon are plotted in Fig. 2 (left). The recombination rate is not shown as it was found, similar to helium, to be much lower than the other two rates. The results show that the charge exchange reaction is expected to occur more often than the ionization, and for plasmoid temperatures on the order of 10 eV or lower the entrainment efficiency may be sufficiently high. For xenon, whose heavy atomic mass implies relatively high thrust levels, the low energy of ionization result in a high rate of electron impact ionization, which for most temperatures of interest is about two orders of magnitude larger than charge exchange rate, thus making the thruster efficiency questionable.

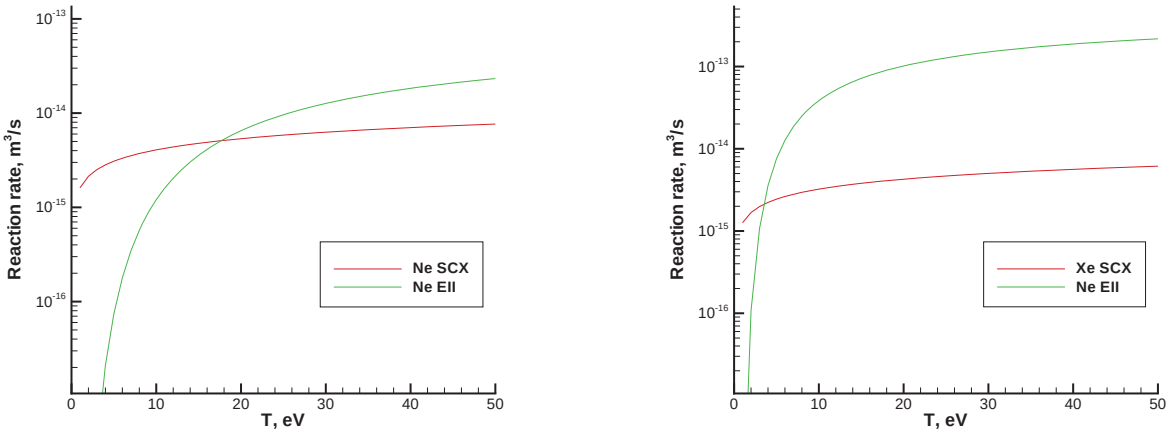

FIGURE 2. Different reaction rates in neon (left) and xenon (right).

HEAT BATH RELAXATION

The plasma relaxation due to the electron impact ionization and charge exchange reactions is a complex process that depends on a number of factors, such as plasma temperature and concentration of reacting species, non-equlibrium of their velocity distributions, and the relashionship between different reaction rates. Let us consider the effect of these factors on the time evolution of plasma and neutral properties in an adiabatic heat bath. Although the spatially homogeneous heat bath can not accurately predict the multi-dimensional evolution of plasma affected by the neutral flow, it nevertheless captures the main features of the relaxation process, and thus helps to understand the relative importance of various factors at play. In order to better reproduce the entrainment process, a finite relative velocity U between plasma (ions and electrons) and neutrals is assumed at time $t = 0$.

The influence of U on the temperature evolution of neutrals, ions, and electrons, is illustrated in Fig. 3 (left). Here and below, the gas is neon, which has the charge exchange reaction rate (see previous section) on the order of the ionization rate, and may therefore be a promising propellant for an FRC thruster. The initial plasma temperature is 10 eV, neutral temperature is 300 K, and both neutral and plasma density are 10^{18} m^{-3}. Consider first the case of 10 km/s. In the absence of relative collision velocity, the ions and neutrals are expected to quickly relax to $0.5*(T_{neut}+T_(ion)\approx 5.01$ eV. The initial relative velocity between ions and neutrals increases this value by about 1.7 eV. The thermal relaxation of electrons due to elastic collisions with neutrals and Coulomb collisions with ions is fairly slow, and the change in electron temperature is primarily related to the electron impact ionization reactions. These endothermic reactions noticeably decrease the electron temperature.

For a relative velocity of 30 km/s, the neutral/ion collisions convert the bulk gas velocity into thermal velocities, which results in strong increase of temperature of these species to over 20 eV. The electron temperature changes very little compared to the 10 km/s case. This is again related to the slow thermal relaxation of electrons, and small change in ionization rate as the relative electron/neutral velocity is small compared to the thermal velocities of electrons, and the latter is the main contributor to ionization. The impact of relative velocity on electron temperature becomes visible only after 100 μs. The important conclusion that can be drawn from these results is that for any flow velocity (and also for any plasma temperature) there is a strong thermal nonequilibrium between neutrals, electrons, and ions. Such a non-equilibrium is expected to occur in the actual neutral entrainment of an FRC thruster, and it requires a kinetic approach to be used for modeling such an entrainment.

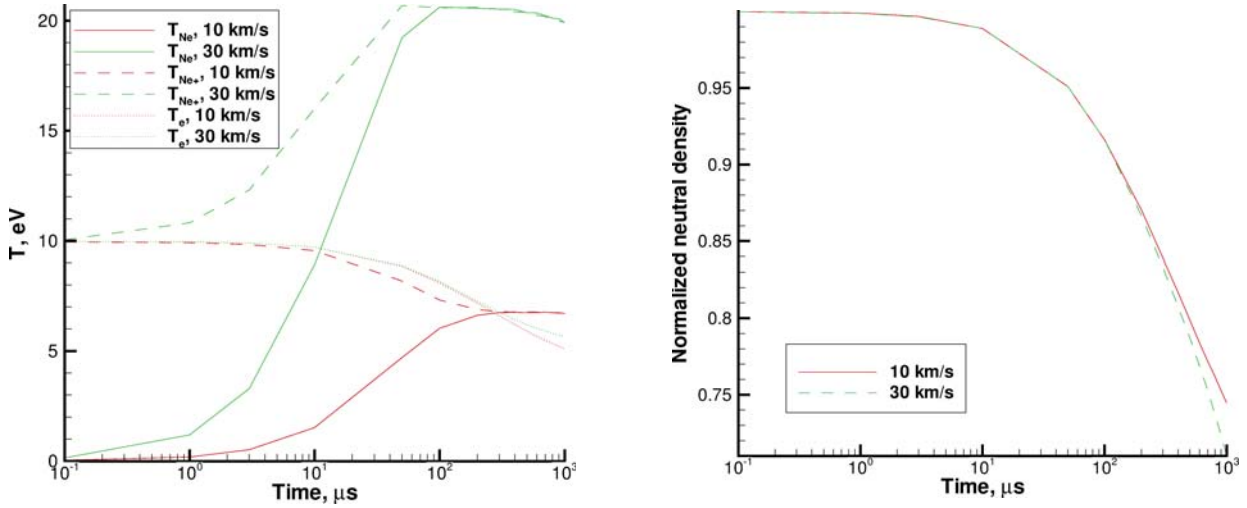

FIGURE 3. Impact of relative velocity on temperature of different species (left) and neutrals density (right) in a heat bath with $T_{p,ini}=10$ eV

The influence of flow velocity on the decrease in neutral number density due to charge exchange and ionization reactions is fairly small, as shown in Fig. 3 (right). For ionization, the reason of such a small influence is given earlier in this section, and for the charge exchange, it is explained by relatively weak dependence of reaction rate on neutral and ion temperature for $T>10$ eV (see Fig. 2) . The initial electron temperature, however, is extremely important, as shown in Fig. 4 (left) for $U=20$ km/s and neutral and plasma number densities of 10^18 m^{-3}. The electron temperature impacts the ionization rate, and when the initial plasma temperature is 50 eV, half of all neutrals are ionized in about 30 μs. The number of charge exchange reactions is about a factor of two lower than ionization reactions for that temperatures. This indicates that the efficiency of an FRC thruster operating at 50 eV will be relatively low. In comparison, for initial plasma temperature of 10 eV, the number of charge exchange reactions is over a factor of five larger than ionization.

The number of charge exchange reactions for a plasma temperature of 10 eV and $U=20$ km/s was found to linearly increase with neutral density when the latter changes from 10^{18} m^{-3} to 3×10^{18} m^{-3}. The dependence of the number of ionization reactions on neutral density is weaker than linear, as can be seen in Fig. 4 (right), where the ion density is given for two values of initial neutral number density. When neutral density increases by a factor three, the ion density increase, primarily affected by the ionization process, is roughly a factor of three only in the first few microseconds. At 1000 μs, the ion density change is only 25% higher than the baseline case. This is primarily related to the depletion of high energy electrons, as will be discussed below.

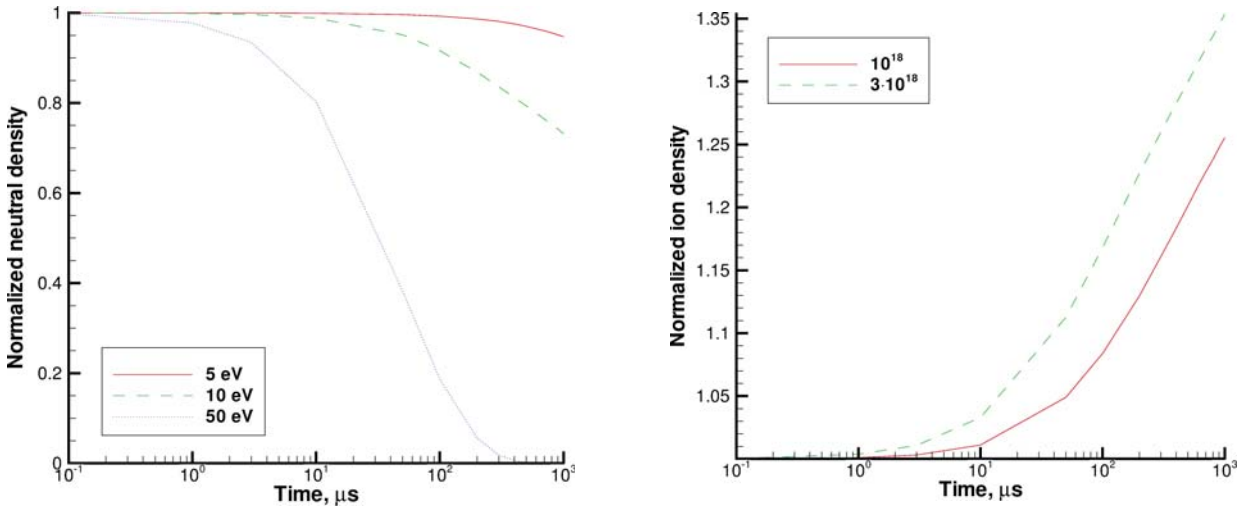

FIGURE 4. Impact of initial plasma temperature (left) and neutrals density (right) on chemical composition.

Generally, the electron impact ionization reactions results in energy transfer from the translational motion of reacting electrons and neutrals to the potential energy of newly formed electron and ion. The reaction therefore decreases plasma temperature, and in particular, depletes the high velocity tail of electrons. This, in turn, will slow down the electron impact ionization rate (but have only limited impact on charge exchange reactions). The main process that leads to the Maxwellization of the electron velocity distribution function is Coulomb collisions between electrons. When the Coulomb collisions are turned off, the high energy tail is quickly depleted by ionization, as illustrated in Fig. 5 (left). There is also noticeable impact of Coulomb collisions on the evolution of plasma density, shown in Fig. 5 (right) for $U = 20$ km/s and $T_{p,ini} = 10$ eV. Note that such a non-equlibrium in velocity distribution is another indication that a kinetic approach is necessary to accurately model neutral entrainment in an FRC thruster. For a multi-dimensional neutral entrainment, when a translated plasmoid passes through neutral gas, the effects mentioned in this section, such as non-equilibrium, fast relaxation rates for high neutral density, strong influence of plasma temperature, the increase of ionization rate due to Coulomb collisions, etc, are expected to be even more pronounced, as the plasma particles collide with new, undisturbed neutral gas due to the plasmoid translation.

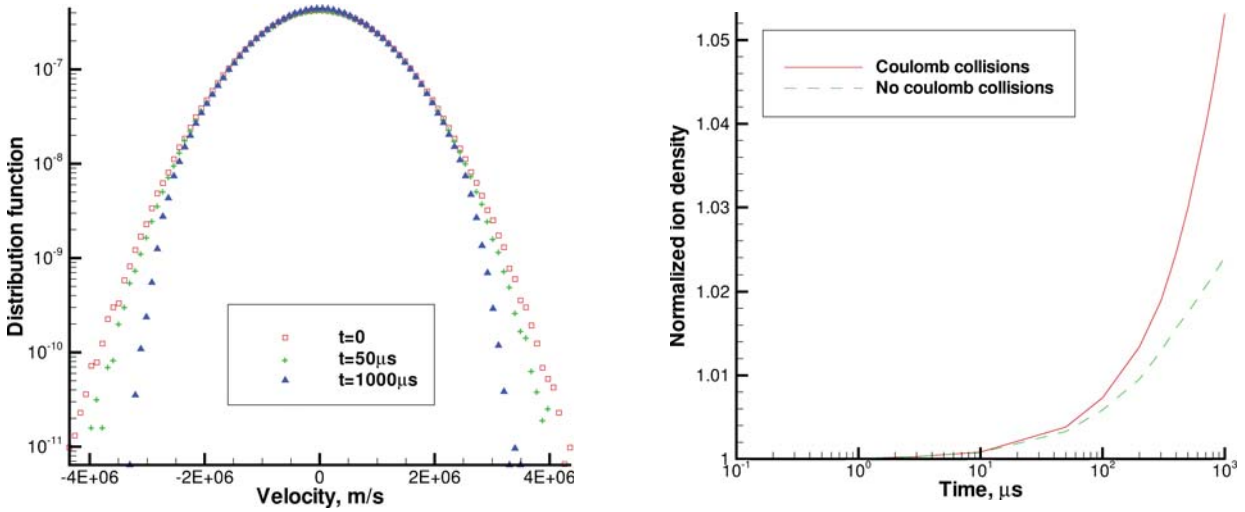

FIGURE 5. Depletion of electron velocity distribution function due to ionization when Coulomb collisions are turned off (left) and the effect of Coulomb collisions on plasma density evolution (right).

FRC NEUTRAL ENTRAINMENT: NUMERCIAL APPROACH AND FLOW CONDITIONS

Celeste3D is used in this work to calculate the interaction between a plasmoid and neutral gas. Celeste3D is an implicit three-dimensional Particle-In-Cell (PIC) code that solves the full set of Maxwell-Vlasov equation and has been extensively used in the past for various astrophysical and laboratory plasma problems.[12, 13] The implicit moment formulation of the PIC method implemented in Celeste results in highly efficient simulations based on ion length and time scales, and not electron scales as explicit methods do, while retaining the kinetic effects of both the electrons and the ions. An explicit simulation requires the time step to be $\Delta t < 2/\omega_{pe}$, and the spatial cell size to be $\Delta x < /\lambda_e$ in order to avoid the finite grid instability. Here, ω_{pe} is the electron plasma frequency, and λ_e is the electron Debye length. In an implicit simulation, these requirements are replaced by an accuracy condition related to the conservation of energy, $\frac{\Delta t < Deltax}{c_e,}$ where c_e is the electron thermal speed.

To simulate the neutral entrainment process, Celeste3D was extended to include neutral particles. A DSMC-based capability has been added to Celeste that includes neutral transport and collisions. The following collision processes are included in this work: neutral-neutral collisions (modeled according to the VHS model [15]); the charge exchange reactions (the cross section is given earlier in this paper); neutral-ion elastic collisions (according to Ref. [10], the cross section is twice the charge exchange cross section); the electron impact ionization (the cross section is also given earlier). The hard sphere after-collision scattering is assumed for all these processes, with the exception of charge exchange reactions, for which the velocities of neutrals and ions are swapped. As all species have different weights, a weighting scheme [16] is applied. The majorant collision frequency [17] of the DSMC method is used to model the collision process in cells. In addition to the neutral capability, a Coulomb collision module has been added to Celeste, based on a particle-weights scheme of Ref. [18].

The computations are performed in 2D (planar flow) in order to increase the number of particles per cell and thus decrease statistical scatter. The grid was 40×80, and the number of simulated ions, electrons, and neutrals per cell was approximately 64, 100, and 512, respectively. Since the cost of an implicit simulation is a direct function of the electron mass (see above, the computational time is inversely proportional to the square root of the electron mass m_e), the simulation efficiency may be further enhanced through the introduction of the weighted electron mass, $m'_e = W m_e$, where the constant $W > 1$. The ion-to-electron mass ratio has to be high enough to preserve the kinetic effects, and the value of m_i/m'_e on the order of 100 is usually sufficient [12]. In this work, $m_i/m'_e = 100$ is used. The initial conditions used to set an equilibrium plasmoid is the a Schmid-Burgk equilibrium [14] with the average plasma density of 10^{18} m^{-3} and a plasma temperature of 10 eV.

For numerical convenience, the neutral-plasma interaction is examined in the reference frame of the plasmoid, so that the neutral gas is injected into the computational domain from the left boundary, and then passes through the domain from left to right. The properties of the injected neutral gas are changed to study their impact on the neutral-plasma interaction. In these computations, periodic boundary conditions for plasma and open boundary conditions for neutrals were imposed at the left and right boundaries, and a conducting wall with specular reflection was set at the top and bottom boundaries. Preliminary computations showed that in the absence of neutrals the equilibrium is maintained for at least 10,000 ion plasma periods (over 30 μs), which is on the order of a typical plasmoid-neutral interaction.

FRC ENTRAINMENT RESULTS

The results of the interaction of an FRC plasmoid with neutral gas are presented in Fig. 6 (left). The figure presents an instanteneous snapshot of ion density at a time of 15 μs after the neutral injection started for all cases except $U = 30$ km/s, for which it is 10 μs after the start of injection (this is the time that the moving neutrals need to cross the computational domain). The ion number density presented in that figure is normalized by 10^{18}. For comparison, the result for a no-neutrals, plasma-only case is also shown (top quarter). Note that the no-neutral field practically does not change with time, with the exception of small changes related to the statistical scatter. The baseline case shown in the second quarter represents the free stream neutral density of 10^{18} and velocity of 20 km/s, and the third and forth cases consider an increased neutral velocity and density, respectively.

For the baseline case, the neutral-plasma interaction results in modest, sligthly more than 5%, increase in the number of ions in the region where the ion density is near its maximum. This is obviously the result of electron impact ionization reactions. It is important to note that there is a clear translation of the plasmoid from the center of the computational domain to the right. The shift, which amounts to almost 2 cm, is due to the momentum transfer from

the moving neutrals to the plasma particles. The average velocity of initially stationary plasmoid is about 3 km/s. Since the computations are conducted in the frame reference of the plasmoid, in application to the actual FRC entrainment configuration that means that the momentum is in fact transferred from the moving plasmoid to the neutral gas. For a higher relative velocity between the plasmoid and netrals, $U = 30$ km/s, the plasma-neutral interaction is clearly weker. The plasmoid is translated only at about 1 cm, and the number of neon ions is increased only by about 3%. The reason for this is a shorter interaction time due to a higher relative velocity between neutral and plasma particles. When the free stream neutral density is increased by a factor of three, the momentum transfer essentially triples, as does the number of inonization reactions. Note also that the strong neutral-plasma interaction results in an elongation of the plasmoid.

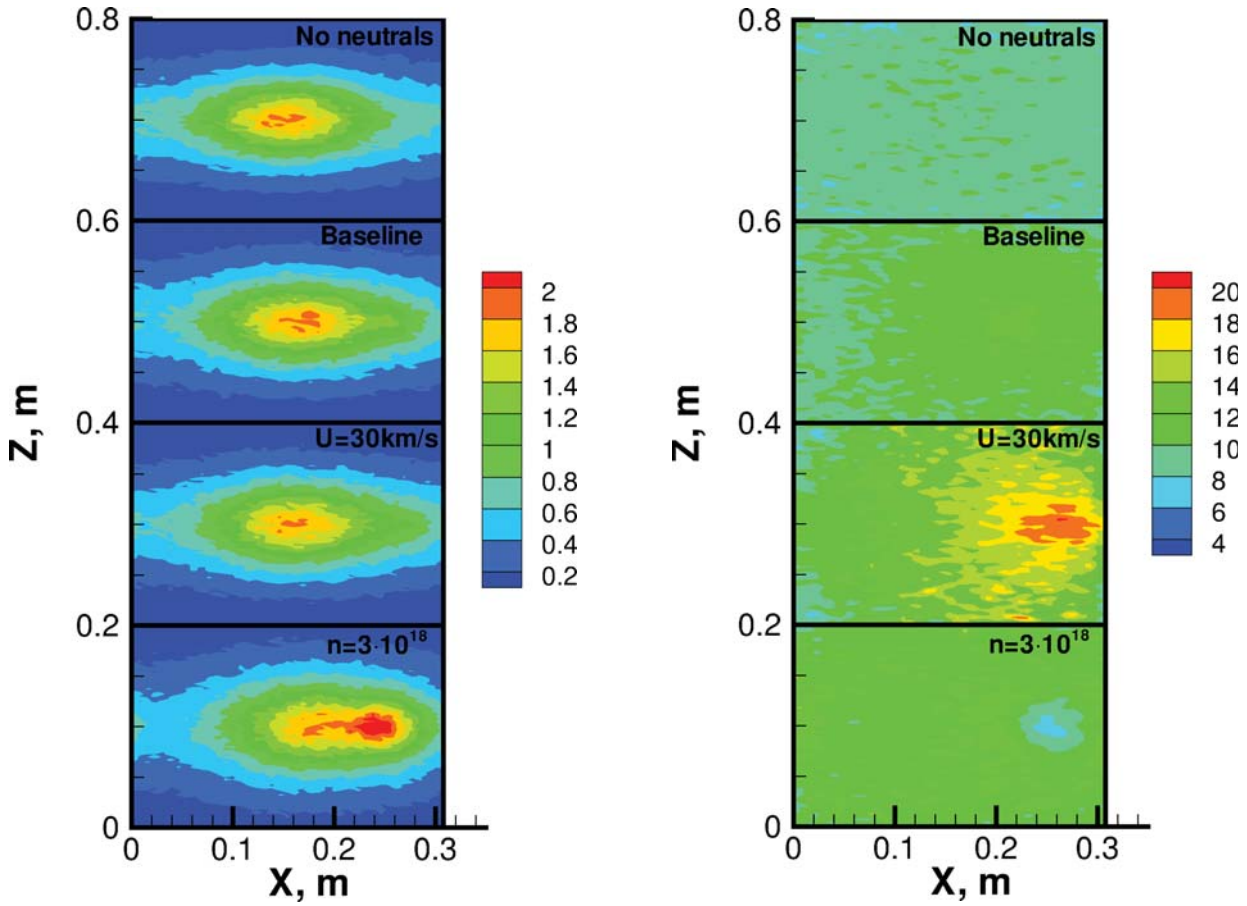

FIGURE 6. Ion density (left) and temperature (right) for different free stream conditions.

For the baseline case, the ion temperature increases by about 1.6 eV in most of the computational domain as compared to the plasma-only case, as illustrated in Fig. 6 right). Here and below, the temperature is in eV. The increase is much more pronounced, over 10 eV, for the $U = 30$ km/s case. This is related to the transfer of energy from the bulk neutral flow motion to the thermal motion of ions and neutrals, and is consistent with the conclusions of the Heat Bath section. Note that for $U = 30$ km/s the maximum ion temperature is observed to the right of the maximum ion density, where more ions have collided with electrons. For the elevated neutral density, there is a minimum ion temperature in this region, related primarily to the large number of endothermic ionization reactions (for the baseline case, there is a temperature minimum in this region, too, although less pronounced). The change in electron temperature (not plotted here) due to entrainment is less significant than for the ion and neutral temperatures (on the order of 10%), as can be expected from Fig. 3 (left).

The number density of neutral particles, normalized by its free stream value, is plotted in Fig. 7 (left). It can be seen that the neutral flow, moving from left to right, almost reached the right boundary of the computational domain. Most importantly, the interaction of neutral particles with ions and electrons depleted their population in the central region by almost 50% for the baseline and elevated density cases, and by over 30% for $U = 30$ km/s. Recalling that

the absolute change in ion density is much smaller than the change in neutral density, it becomes clear that the latter is related to charge exchange reactions. The neutral particles loose there momentum in X direction after charge exchange reactions, and thus do not reach the right boundary. The temperature field of neutral particles, shown in Fig. 7 (right), indicates the region where neutrals mostly travel after they are created as a result of charge exchange reactions. It is the region of elevated temperature (relative velocity between these neutrals and free stream neutrals is high) observed mostly to the left of the center of the plasmoid, and away from the top and bottom conducting walls. Therefore, in the actual entrainment the neutrals are expected to travel with the plasmoid.

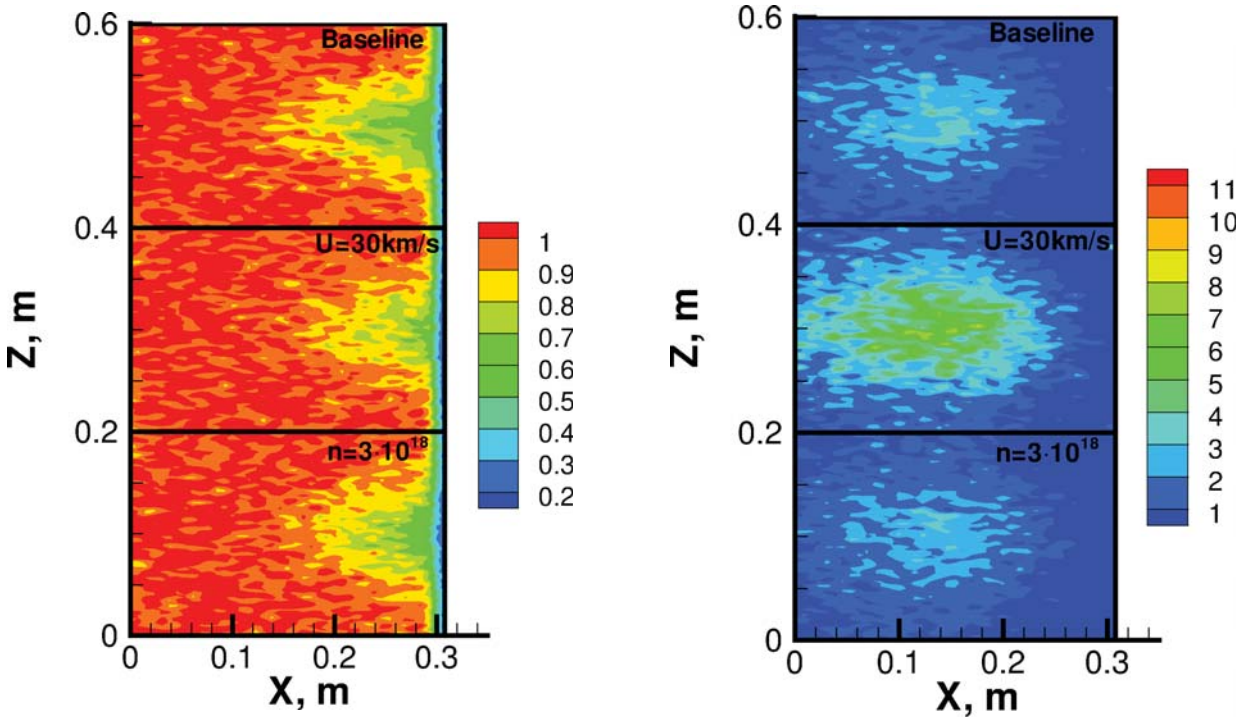

FIGURE 7. Neutral density (left) and temperature (right) for different free stream conditions.

CONCLUSIONS

The numerical analysis is conducted of interaction between a translated field reversed configuration plasmoid and neutral gas. The interaction models the neutral entraiment observed in FRC thrusters and is characterized by a number of chemical and thermal processes, among which the charge exchange and electron impact ionization reactions are most important. While the former increases thrust and improves total efficiency of an FRC thruster, the latter is expected to decrease them. Comparison of ionization and charge exchange reaction rates indicates that the use of nitrogen and xenon may be problematic, while neon appears to be a fairly good propellant.

Thermal relaxation in an adiabatic heat bath was modeled for neutral and plasma parameters that are expected in FRC thrusters. It has been shown that the relaxation process proceeds under conditions of strong thermal and chemical nonequilibirum; ion, electron, and neutral temperatures strongly differ, and the electron distribution function is non-Maxwellian. This indicates that a kinetic approach has to be used to model neutral entrainment in FRC thrusters. Strong impact of electron temperature on plasma density is shown in heat bath relaxation, mostly related to ionization reactions. Increase in relative velocity between plasma and neutrals strongly affects ion and neutral temperature. Electron impact ionization was found to deplete high velocity tail of the electron distribution function, and modeling of Coulomb collisions between electrons is necessary to properly account for that depletion. The electron-neutral and electron-ion thermal relaxation, according to the present computations, is not expected to be a factor in neutral entrainment process.

The simulation of a planar interaction between an FRC plasmoid and neutral gas is conducted with an implicit PIC code Celeste3D, extended in this work to include neutral transport, plasma-neutral and neutral-neutral collisions

and Coulomb collisions. Neon propellant was used with a baseline plasma and neutral densities of 10^{18} m^{-3}, plasma temperature of 10 eV, and relative velocity of 20 km/s. The modeling results show strong entrainment of neutral particles by a translated plasmoid as a result of charge exchange reactions between slow neutrals and fast moving ions, and a modest increase in plasma density due to electron impactg ionization. The increase in neutral density appears highly beneficial in terms thruster efficiency as it proportionally increases the number of entrained neutrals. The increase in plasmoid velocity decreases that number due to a shorter plasma-neutral interaction time.

ACKNOWLEDGMENTS

The work was supported by the Air Force Office of Scientific Research and the Propulsion Directorate of the Air Force Research Laboratory at Edwards Air Force Base California.

REFERENCES

1. McKenna K.F. et al., "Particle confinement scaling in field-reversed configurations", Phys. Rev. Lett. 50, 1787 (1983)
2. Rostoker N. and Qerushi A., "Classical transport in a field reversed configuration", Plasma Phys. Rep. 29(7), 626 (2003).
3. Elliott F., Foster J., and Patterson M., An Overview of the High Power Electric Propulsion (HiPEP) Project, AIAA Paper 2004-3453.
4. Kirtley D., Brown D., and Gallimore A. Details on an annular field reversed configuration plasma device for spacecraft propulsion, IEPC-2005-171.
5. Miller S., Rovey J. Progress in modeling of pre-ionization and geometric effects on a field-reversed configuration plasma thruster, AIAA 2009-3733.
6. Slough J., Kirtley D., and Weber T. Pulsed plasmoid propulsion: the ELF thruster, IEPC-2009-265.
7. Lapenta, J.U. Brackbill, Dynamic and Selective Control of the Number of Particles in Kinetic Plasma Simulations, Journal of Computational Physics, 115, 213-227, 1994.
8. Kirtley, D., Slough, J., Pihl, C., Meier, E., Milroy, R., Pulsed plasmoid propulsion: airbreathing electromagnetic propulsion, IEPC-2011-015.
9. l. C. Pitchford, J. P. Boeuf, and W. L. Morgan, User-friendly Boltzmann code for electrons in weakly ionized gase, in Proceedings of the IEEE International Conference on Plasma Science, Boston, MA, 1996 (IEEE, Piscataway, NJ, 1996).
10. S.A. Losev, S.O. Macheret, B.V. Potapkin, G.G. Chernyi, Physical and chemical processes and gas dynamics: cross sections and rate constants. Progress in Astronautics and Aeronautics, 196, AIAA, 2002.
11. Raizer Yu.P., Gas discharge physics, Springer-Verlag, Berlin Heidelberg, 1991
12. P.Ricci, G. Lapenta, J.U. Brackbill, GEM Challenge: Implicit Kinetic Simulations with the Physical Mass Ratio, Geophysical Research Letters, 29, 10.1029/2002GL015314, 2002.
13. Lapenta, G., Brackbill, J. and Ricci, P. Phys. Plasmas 13, 055904 (2006).
14. Schmid-Burgk, J. Finite Amplitude Density Variations in a Self-Gravitating Isothermal Gas Layer, Astrophysical Journal, vol. 149, 727-729 (1967).
15. Bird, G.A., *Molecular Gas Dynamics and the Direct Simulation of Gas Flows.* Clarendon Press, Oxford. 458 pp, 1994.
16. Gimelshein S.F., Levin D.A., Collins R.J. Modeling of Infrared Radiation in a Space Transportation System Environment. AIAA Journal, Vol. 40, No. 4, 2002, pp. 781-790.
17. Ivanov, M.S. and Rogasinsky, S.V., Analysis of the numerical techniques of the direct simulation Monte Carlo method in the rarefied gas dynamics, *Soviet J. Numer. Anal. Math. Modeling*, Vol. 3, No. 6, 1988, pp. 453-465.
18. K. Nanbu and S. Yonemura, Weighted Particles in Coulomb Collision Simulations Based on the Theory of a Cumulative Scattering Angle J. Comp. Phys, 145, 639-654 (1998)